2. A. Galvanauskas, M. E. Fermann, D. Harter, J. D. Minelly, G. G. Vienne, J. E. Caplen, in *Conference on Lasers and Electro-Optics*, vol. 9 of 1996 OSA Technical Digest Series (Optical Society of America, Washington, D.C., 1996), pp. 495–496.
3. A. Galvanauskas, P. A. Krug, D. Harter, Opt. Lett. **21,** 1049 (1996).
4. L. E. Myers, R. C. Eckardt, M. M. Fejer, R. L. Byer, W. R. Bosenberg, J. W. Pierce, J. Opt. Soc. Am. B **12,** 2102 (1995).
5. V. Pruneri, J. Webjorn, P. St. Russell, D. C. Hanna, Appl. Phys. Lett. **67,** 2126 (1995).
6. A. Galvanauskas, M. A. Arbore, M. M. Fejer, M. E. Fermann, D. Harter, to be published in Opt. Lett.
7. G. P. Banfi, C. Solcia, P. Di Trapani, R. Danielius, A. Piskarskas, R. Righini, R. Torre, Opt. Commun. **118,** 353 (1995).

CThH4 **11:30 am**

Self-tuning in additive-pulse modelocked fiber lasers using Bragg gratings

D. W. Huang, S. Y. Liang, Y. W. Kiang, C. C. Yang, *Institute of Electro-Optical Engineering and Department of Electrical Engineering, National Taiwan University 1, Roosevelt Road, Sec. 4, Taipei, Taiwan, R.O.C.; E-mail: ccy@cc.ee.ntu.edu.tw*

It is well known that the additive-pulse modelocking (APM) technique requires that the optical path difference between the two coupled cavities must be controlled within a wavelength-order accuracy to achieve the interferometric APM action. Recently, self-tuned coupled-cavity passively modelocked fiber lasers were reported.[1] These lasers used three fiber Bragg gratings to form the coupled cavities. Stable modelocked pulses were observed without wavelength-order cavity length control. This implies that the APM that uses gratings to form coupled cavities can be quite simple. However, the physical reason for the APM without good cavity length control has not been understood yet. In this paper, we report our discovery that the wavelength-dependent delay property of Bragg gratings is the origin of the self-tuning mechanism. The reflection coefficient $r(\omega)$ and transmission coefficient $t(\omega)$ of a fiber Bragg grating are

$$r(\omega) = -j\kappa\sinh(L\sqrt{\kappa^2-\delta^2})/[\sqrt{\kappa^2-\delta^2}\cosh(L\sqrt{\kappa^2-\delta^2}) + j\delta\sinh(L\sqrt{\kappa^2-\delta^2})], \quad (1)$$

$$t(\omega) = \sqrt{\kappa^2-\delta^2}/[\sqrt{\kappa^2-\delta^2}\cosh(L\sqrt{\kappa^2-\delta^2}) + j\delta\sinh(L\sqrt{\kappa^2-\delta^2})], \quad (2)$$

where L is the length of the grating, κ is the coupling coefficient, and δ is the phase mismatching, i.e., $\delta = \beta(\omega)-\beta_0 \approx \beta_0'(\omega-\omega_0) = (\omega-\omega_0)/V_g$, where $V_g = 1/\beta_0'$ is the group velocity. We assume that $\kappa = 400$ rad/m, three fiber Bragg gratings with lengths $L_1 = 10$ mm, $L_2 = 4.6$ mm, and $L_3 = 3.5$ mm (see Fig. 1 for the laser configuration). Also, the center wavelengths of these gratings are the same (centered at 1.55 μm) and the bandwidths of the reflectivity curves are around 0.5 nm. The nonlinear dependencies of the phases of the reflection coefficients on wavelength mean that pulses with different center wavelengths experience different delay times when reflected by a grating. The delay time $T_d(\omega)$ is the derivative of the phase as

$$T_d(\omega) = -\frac{d}{d\omega}\phi_r(\omega) = \frac{\kappa^2\cosh(L\sqrt{\kappa^2-\delta^2})\sinh(L\sqrt{\kappa^2-\delta^2}) - L\delta^2\sqrt{\kappa^2-\delta^2}}{\sqrt{\kappa^2-\delta^2}[\kappa^2\cosh^2(L\sqrt{\kappa^2-\delta^2}) - \delta^2]}\cdot\frac{1}{v_g}. \quad (3)$$

We define an effective penetration length into the grating as $\Delta L_{\text{eff}}(\omega) = V_g T_d(\omega)/2$. In Fig. 2, the effective penetration lengths of the three Bragg gratings are plotted. In this coupled-cavity APM system, the cavity mismatch can be tolerated by the difference of the effective penetration lengths between the gratings at the two ends. Because the center grating causes equal delay times in the two coupled cavities, it makes no contribution in compensating for cavity mismatch. In the inset of Fig. 2, the difference of the effective penetration length between the two end gratings is shown. In the spectral range from 1549.8 to 1550.2 nm, this length difference is between 0.06 and 5 mm. If the physical mismatch of the coupled cavities is 0.2 mm, it can be compensated by shifting the center wavelength from 1550 to 1550.11 nm. We conducted a numerical simulation of this coupled-cavity APM fiber laser system. By shifting the center wavelength, we can obtain a typical APM action that leads to pulse shortening (Fig. 3). Therefore, Bragg gratings in an in-line coupled-cavity fiber laser act as wavelength-dependent delay lines. The length mismatching of the coupled cavities can be automatically compensated through Bragg gratings and wavelength-order cavity control is unnecessary.

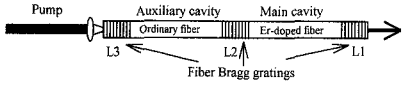

CThH4 Fig. 1 Experimental setup for an in-line coupled-cavity APM fiber laser.

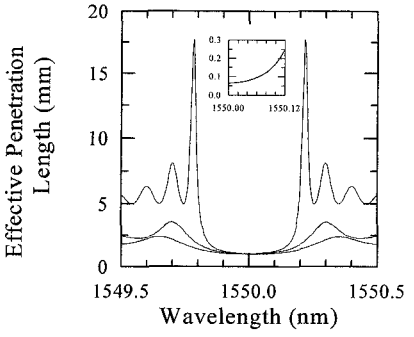

CThH4 Fig. 2 Effective penetration lengths of the three fiber Bragg gratings. The inset shows the difference of effective penetration length between the two end gratings.

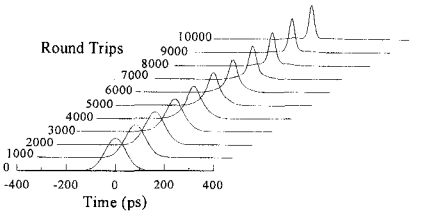

CThH4 Fig. 3 Pulse shortening in the in-line coupled-cavity APM fiber laser.

We wish to acknowledge support by the National Science Council under the grants NSC 85-2115-E-002-003, NSC 85-2115-E-002-004 and NSC 85-2115-E-002-010.

1. P. K. Cheo, L. Wang, M. Ding, IEEE Photon. Technol. Lett. **8,** 66 (1996).

CThH5 **11:45 am**

Modelocking pulse dynamics in fiber lasers

J. Nathan Kutz,* Keren Bergman,** S. Tsuda,† Wayne H. Knox,† *Program in Applied Mathematics, Princeton University, Princeton, New Jersey 08544; E-mail: kutz@math.princeton.edu*

Erbium-doped modelocked fiber lasers provide a potentially attractive short pulse source[1] near 1.5 microns for applications to high speed fiber optic communication systems and interconnection networks. A recently developed semiconductor saturable absorber device at Lucent Technologies incorporates an epitaxially grown pair of InGaAs quantum wells and a low loss, broadband Bragg reflector structure to produce a saturable Bragg reflector (SBR).[2] This nonlinear mirror has been used to passively modelock erbium-doped fiber lasers near 1.5 microns.[3] These results are promising for high-speed TDM/WDM networks that require broadband and stable sources.

In this paper we present theoretical and numerical studies of the modelocked fiber cavity including a description of the pulse formation dynamics and its interaction with the SBR. Our model begins with the pulse propagating in an optical fiber under the influence of the Kerr nonlinearity and including the effects of dispersion, loss, and a parabolic gain bandwidth profile. Thus the pulse evolves according to the modified nonlinear Schrödinger equation

$$i\frac{\partial Q}{\partial Z} + \frac{D}{2}\frac{\partial^2 Q}{\partial T^2} + \alpha|Q|^2Q + i\Gamma Q - iG(Z) \times\left(1+\tau\frac{\partial^2}{\partial T^2}\right)Q = 0, \quad (1)$$

where Q is the normalized electric field envelope and D, α, τ, and Γ denote the normalized dispersion, nonlinearity, gain bandwidth, and intrinsic loss, respectively.

The SBR is modeled with three separate time constants: an instantaneous response (AC stark), a slow saturated response (real carrier transitions), and a relaxation time. The ana-

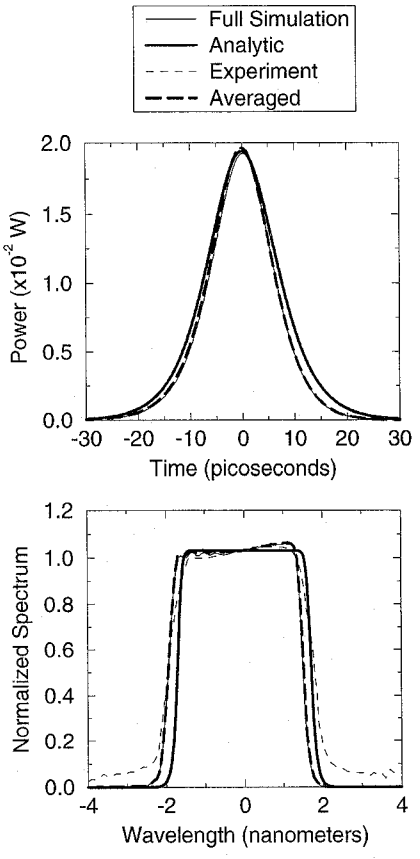

CThH5 Fig. 1 Comparison of the experimental results in the normal dispersion regime with numerical simulations of the full evolution equations, the averaged equation, and the approximate analytic solution.

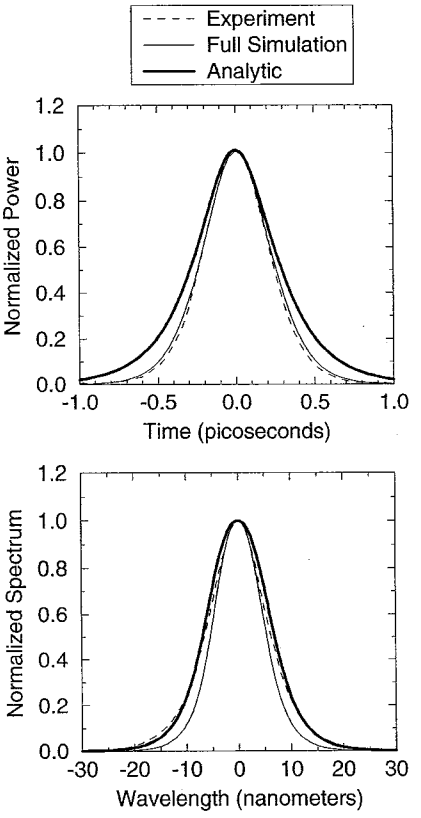

CThH5 Fig. 2 Comparison of the experimental results in the anomalous dispersion regime with numerical simulations of the full evolution equations and the approximate analytic solution.

lytical model for the temporal response of the SBR matches closely experimental measurements obtained via pump-probe experiments. The SBR and output coupler (OC) are both treated as jump conditions to the propagation Eq. (1) so that

$$\text{at SBR:} \quad Q_+ = f(|Q|)Q_- \qquad (2a)$$

$$\text{at OC:} \quad Q_+ = RQ_- , \qquad (2b)$$

where $Q_\pm$ denotes the pulse before $(-)$ and after $(+)$ the SBR or OC interaction, $f(|Q|)$ is the intensity-dependent temporal response of the SBR, and R is the reflectivity of the OC. This modelocking model can be simulated numerically to accurately predict the output temporal and spectral pulse profiles obtained experimentally. In addition, we derive an averaged model that captures the effect of the SBR dynamics and can be solved analytically. This model is significantly different than the master modelocking equation used previously to describe modelocked lasers.[4]

We compare the numerical simulations of the full evolution equations and averaged evolution with the analytical results and experimental findings for laser operation in both the normal (see Fig. 1) and anomalous (see Fig. 2) dispersion regimes. Remarkable quantitative agreement is achieved in the normal dispersion regime as illustrated in Fig. 1. However, the model requires a significant increase in the fast response (SBR) parameter to correctly capture the evolution of the subpicosecond, highly intense pulses observed in the anomalous dispersion regime. The modifications, which help attenuate the growth of temporal side lobes generated from the strong self-phase modulation in the cavity, can be incorporated and are shown to give excellent agreement with experimental predictions. This is depicted in Fig. 2. The disagreement in the anomalous regime cannot be explained by soliton modelocking.

*Also with Lucent Technologies and AT&T Research, Murray Hill, New Jersey 07974

**Department of Electrical Engineering and Advanced Technology Center for Photonics and Opto-Electronic Materials, Engineering Quadrangle, Princeton University, Princeton, New Jersey 08544;
E-mail: bergman@ee.princeton.edu

†Lucent Technologies, Bell Laboratories, Holmdel, New Jersey 07733;
E-mail: wknox@lucent.com

1. I. N. Duling, III, M. L. Dennis, *Compact Sources of Ultrashort Pulses* (Cambridge University Press, Cambridge, 1995).
2. S. Tsuda, W. H. Knox, E. A. de Souza, W. Y. Jan, J. E. Cunningham, Opt. Lett. **20,** 1406–1408 (1995).
3. S. Tsuda, W. H. Knox, J. L. Zyskind, J. E. Cunningham, W. Y. Jan, R. Pathak, Paper CFD2, Conference on Lasers and Electro-Optics, Anaheim, Calif. 1996.
4. H. A. Haus, J. G. Fujimoto, E. P. Ippen, J. Opt. Soc. Am. B **8,** 2068–2076 (1991).

CThI

10:30 am–12:00 m
Rooms 321/323

Transmission Systems

Curtis R. Menyuk, *University of Maryland–Baltimore Co., Presider*

CThI1 (Invited) **10:30 am**

Advances in repeaterless transmission systems

P. B. Hansen, *Bell Laboratories, Lucent Technologies, 101 Crawfords Corner Road, Holmdel, New Jersey 07733*

In the course of only a couple of years the maximum reported transmission distance for a 2.5-Gb/s repeaterless system increased from 347 km to 529 km while the corresponding power budget increased to 93.8 dB.[1–15] The progress was equally dramatic for 10-Gb/s systems. In 1993 the maximum reported transmission distance and power budget were 300 km and 61.9 dB, respectively.[16] By 1996 a distance of 442 km and a power budget of 81.5 dB had been achieved.[17] Experiments have also shown that wavelength division multiplexing is an attractive means for increasing the capacity at a modest cost in terms of reduced transmission distance (e.g., Refs. 18–23).

Figure 1 depicts the 529-km, 2.5-Gb/s experimental repeaterless transmission system that will be used to discuss the recent advances in the field.[11] This implementation includes Raman amplification as well as remote post- and pre-amplifiers pumped partly via the transmission fiber and partly via dedicated pump fibers by 1480-nm pump sources providing powers up to 1.3 W.[24] The transmission fiber, into which 26.5 dBm is launched, consists of dispersion-shifted fiber with a high zero-dispersion wavelength combined with low-loss silica-core fiber. Furthermore, dispersion compensation (e.g., Refs. 25–31) and forward error correction are employed.[32]

Repeaterless transmission systems have benefited from advances in a number of technologies—first and foremost from the advent of high-power diode-pumped laser sources with wavelengths near 1480 nm (e.g., Refs. 24,33). A very rapid ten-fold increase in the available power made remote pumping of erbium-doped fibers as well as Raman amplification attractive. Power budget improvements up to 18.9 dB were obtained by incorporating remotely pumped pre-amplifiers.[11] These were pumped through the transmission fiber and, in some experiments, also via dedicated pump fibers. Raman gain combined with Rayleigh back scattering acting on the signal in the transmission fiber as well as Raman down shifting of the pump light in the dedicated pump fiber ultimately limits the possible power budget increase. Remotely pumped post-amplifiers offer fewer, typically single-digit, dB's for the same pump power as the